



This is a repository copy of *A method to evaluate the degree of bleaching of IRSL signals in feldspar: The 3ET method.*

White Rose Research Online URL for this paper:
<https://eprints.whiterose.ac.uk/188131/>

Version: Published Version

Article:

Ivester, A.H., Rhodes, E.J. orcid.org/0000-0002-0361-8637, Dolan, J.F. et al. (5 more authors) (2022) A method to evaluate the degree of bleaching of IRSL signals in feldspar: The 3ET method. *Quaternary Geochronology*, 72. 101346. ISSN 1871-1014

<https://doi.org/10.1016/j.quageo.2022.101346>

Reuse

This article is distributed under the terms of the Creative Commons Attribution (CC BY) licence. This licence allows you to distribute, remix, tweak, and build upon the work, even commercially, as long as you credit the authors for the original work. More information and the full terms of the licence here:
<https://creativecommons.org/licenses/>

Takedown

If you consider content in White Rose Research Online to be in breach of UK law, please notify us by emailing eprints@whiterose.ac.uk including the URL of the record and the reason for the withdrawal request.



eprints@whiterose.ac.uk
<https://eprints.whiterose.ac.uk/>



A method to evaluate the degree of bleaching of IRSL signals in feldspar: The 3ET method

A.H. Ivester^{a,*}, E.J. Rhodes^a, J.F. Dolan^b, R.J. Van Dissen^c, J. Gauriau^b, T. Little^d, S.F. McGill^e, P.A. Tuckett^a

^a Department of Geography, The University of Sheffield, Sheffield, S10 2TN, United Kingdom

^b Department of Earth Sciences, University of Southern California, Los Angeles, CA, USA

^c GNS Science, Lower Hutt, New Zealand

^d School of Geography, Environment, and Earth Sciences, Victoria University of Wellington, New Zealand

^e Department of Geological Sciences, California State University, San Bernardino, CA, USA

ARTICLE INFO

Keywords:

Luminescence dating
pIR-IRSL
3ET
Bleaching

ABSTRACT

In addition to dating, IRSL luminescence signals can preserve information about erosional, transport, and depositional histories of a population of grains. Knowledge of the degree of bleaching can be useful in understanding the processes that occurred during previous depositional events, as certain transport conditions result in a well bleached signal, while others result in grains retaining an inherited signal from prior events. This information can be accessed by making single-grain IRSL measurements across successively increasing temperatures, thereby isolating signals from traps of different bleachabilities.

A new approach offers a way to evaluate the completeness of bleaching of a grain by testing patterns of equivalent dose (D_E) values measured at three elevated temperatures (3ET), 50, 125, and 225 °C. Consistent D_E estimates across two or more temperatures suggest a single bleaching event of sufficient duration to fully depopulate the traps involved. Incompletely bleached grains with inconsistent D_E values across temperatures will lack a 3ET “plateau.” Modes in the distribution of D_E values for fully bleached grains can suggest depositional ages, subject to assessment of fading. We developed a Python code in a Jupyter Notebook environment for data analysis and visualization to expedite processing the large data sets produced by the 3ET protocol.

The 3ET protocol was tested on a radiocarbon dated sequence of playa samples from California, USA and on a set of fluvial terraces in the Marlborough region of New Zealand as part of a larger project to reconstruct regional seismic history. Where standard pIRIR apparent ages can be inconsistent or ambiguous, 3ET age estimates produce generally consistent apparent ages. Modes of 3ET plateaus can be used to infer the most recent and prior events that resulted in a sub-population of grains being fully bleached. These initial results suggest that the 3ET method can be useful to characterize both the age and degree of bleaching of depositional events.

1. Introduction

Methods have been developed previously to isolate a luminescence signal from feldspars that is useful for dating sediments and more stable than the infra-red stimulated luminescence (IRSL) decay measured at 50 °C (Buylaert et al., 2009). These methods are based on a single aliquot regenerative-dose (SAR) protocol and follow a similar approach as post-IR OSL dating of fine-grained polymineral samples (Banerjee et al., 2001). Two principal dating protocols were introduced that build on many systematic studies of feldspar IRSL measured at raised

temperatures following an initial IRSL “wash” at 50 °C (e.g., Thomsen et al., 2008). The pIRIR₂₂₅ procedure incorporates a second IRSL measurement at 225 °C with a 60s preheat at 250 °C (Buylaert et al., 2009) and the pIRIR₂₉₀ procedure with a second IRSL at 290 °C and a 60s preheat at 320 °C (Buylaert et al., 2012). Standard pIRIR₂₂₅ protocols applied to feldspar grains can work very well (e.g., Reimann et al., 2011), yielding age estimates consistent with those from independent methods. However, in some settings, samples suffer from incomplete bleaching due to short transport distance, rapid erosion and re-burial, or limited sunlight exposure due to other factors such as terrain, latitude,

* Corresponding author.

E-mail address: a.ivester@sheffield.ac.uk (A.H. Ivester).

<https://doi.org/10.1016/j.quageo.2022.101346>

Received 1 December 2021; Received in revised form 20 May 2022; Accepted 23 May 2022

Available online 27 May 2022

1871-1014/© 2022 The Authors. Published by Elsevier B.V. This is an open access article under the CC BY license (<http://creativecommons.org/licenses/by/4.0/>).

Table 1

Luminescence sample descriptions. The four samples from the El Paso Peaks site are from playa sediments, collected from a single trench. For full context and stratigraphy of the numbered stratigraphic units at the El Paso Peaks site, see Dawson et al. (2003). The twelve samples from McLean Stream valley are alluvial deposits collected from the modern channel and from three terraces, with relative heights above the modern channel as indicated.

Lab ID	Field Code	Site ^a	Depth (cm)	Description
J0140	EPP11-04	EPP	93	Playa sediments; Stratigraphic unit 100
J0145	EPP11-09	EPP	168	Playa sediments; Stratigraphic unit 128b
J0150	EPP11-14	EPP	213	Playa sediments; Stratigraphic unit 144
J0156	EPP11-20	EPP	434	Playa sediments; Stratigraphic unit 270
Shfd19126	KE19-15	MSV	0–14	Modern stream channel
Shfd19127	KE19-16	MSV	35	Low terrace
Shfd19128	KE19-17	MSV	300	Low terrace
Shfd19129	KE19-18	MSV	360	Low terrace
Shfd19130	KE19-19	MSV	425	Low terrace
Shfd19131	KE19-20	MSV	107	Middle terrace
Shfd19132	KE19-21	MSV	172	Middle terrace
Shfd19133	KE19-22	MSV	187	Middle terrace
Shfd19134	KE19-23	MSV	220	Middle terrace
Shfd19135	KE19-24	MSV	75	High terrace
Shfd19136	KE19-25	MSV	112	High terrace
Shfd19137	KE19-26	MSV	115	High terrace

^a EPP = El Paso Peaks, California, USA; MSV = McLean Stream valley, South Island, New Zealand.

or transport in deep or turbid water (Smedley et al., 2019). In these settings, single grain approaches using a pIRIR₂₂₅ protocol can often overcome these problems (Reimann et al., 2012; Rhodes, 2015; Smedley and Duller, 2013). Where samples in addition suffer from in-mixing of young grains from overlying horizons or the surface by bioturbation, or where very poor bleaching leaves only a small fraction apparently consistent, ambiguities in the interpretation of single grain pIRIR datasets can still exist. In order to assess IRSL signal thermal stability for dating loess sequences, Li and Li (2011) introduced a multiple temperature multi measurement IRSL approach, subsequently referred to as multiple elevated temperature (MET-) IRSL, though other names are sometimes applied to similar techniques. Reimann et al. (2015) used such an approach for testing the completeness of bleaching for fine-grained polymineral samples, and Fu and Li (2013) used a similar approach for dating conventional multiple-grain feldspar aliquots from Holocene sediments. A MET-IRSL protocol that used the same preheating treatment as the pIRIR₂₂₅ protocol was developed and applied to single grains of K-feldspar by McGuire and Rhodes (2015) in order to track patterns of sediment transport within the Mojave River, California, USA.

To overcome problems of severe incomplete bleaching, and to avoid “shadowing”, an effect where a significant population of reworked grains with higher dose values make the identification of the smaller number of well bleached grains challenging (Rhodes and Walker, 2019), a new protocol has been developed that compares results from multiple signals within individual single grains to identify only those that are well bleached. This approach takes advantage of the differential bleachability of IRSL signals measured at three different temperatures: 50, 125, and 225 °C, hence the name 3ET (three elevated temperatures). It has some of the advantages of MET-IRSL (e.g., Reimann et al., 2015), along with those offered by single grains (Reimann et al., 2012; Rhodes 2015), without being as time consuming as a single grain MET-IRSL protocol. The selection of IRSL measurement temperatures allows us to maintain the 60s, 250 °C preheat from the well-tested single grain pIRIR₂₂₅ protocol (Rhodes and Walker, 2019). Colarossi et al. (2018) and Kars et al. (2014b) provide useful advice concerning the selection of preheat conditions, and other aspects of post-IR IRSL protocol design.

Table 2

Three elevated temperature (3ET) IRSL single aliquot regenerative-dose (SAR) protocol.

Step	Each SAR 3ET cycle comprises:
1	Natural or laboratory beta dose
2	Preheat 60s 250 °C 5 °C s ⁻¹
3	SG IR Laser 50 °C 2.5s 90% power
4	SG IR Laser 125 °C 2.5s 90% power
5	SG IR Laser 225 °C 2.5s 90% power
6	Beta test dose 8 Gy
7	Preheat 60s 250 °C 5 °C s ⁻¹
8	SG IR Laser 50 °C 2.5s 90% power
9	SG IR Laser 125 °C 2.5s 90% power
10	SG IR Laser 225 °C 2.5s 90% power
11	IR LED Hot Bleach 290 °C 100s 90% power

In this paper we assess the 3ET method to evaluate potential benefits, limitations, and other considerations in its application. First, we compare 3ET age estimates for desert playa sediments dated independently by radiocarbon. Secondly, we examine internal consistency of 3ET results for a suite of terraces along a high-energy braided stream with suboptimal bleaching conditions.

2. Sample description

A total of sixteen luminescence samples were collected from two sites to test the 3ET method (Table 1). Four samples were collected from a detailed paleoseismic trench near El Paso Peaks, California. Previously determined radiocarbon ages from this site are ideal for the purposes of assessing luminescence protocols; from 30 detrital charcoal age estimates measured at the site, 25 form a highly coherent age sequence ranging from the present day back to 7000 years before present and were used to construct a comprehensive Bayesian age model (Dawson et al., 2003). These authors recorded the stratigraphy in detail, and the original excavation face was clearly visible when the site was reopened to collect luminescence test samples in 2011 (Roder et al., 2012). One of the original excavation team helped reopen the trench, and we had access to the original large scale section logs as we sampled for luminescence. The site represents a small playa lake impounded by a shutter ridge formed by slip on the Garlock fault, into which silty to gravelly fluvial deposits were introduced, providing the opportunity to assess both low and higher energy deposits.

The remaining twelve luminescence samples in this present study are from a suite of fluvial terraces alongside McLean Stream, a tributary to the Clarence River on the South Island of New Zealand. These samples can be used to test for internal consistency of the 3ET method as the ages should be older for successively higher terraces. These two sites represent extremes in expected bleaching conditions: a sunny, low-energy desert playa environment with high bleaching potential (El Paso Peaks) and a high-energy, braided fluvial system in an active tectonic region with limited opportunities for thorough bleaching (McLean Stream terraces).

3. Methods

Luminescence samples were collected in the field in aluminum tubes (5 cm-diameter by 15 cm-length), with light-proof caps. Under red or amber light in the laboratory the caps and ~3 cm from the tube ends were removed to be used for moisture content determination. A subsample was obtained with a sample splitter and milled to a fine powder for ICP determination of U, Th, and K-40. Dose rate determination was based on ICP values and field gamma spectrometry measurements. Sediment from the tube interiors was wet-sieved to retain the 90–250 μm fraction. This was treated to remove any carbonate with 1M HCl, rinsed, then treated with H₂O₂ (30%) to remove organic matter and given a final rinse. The dried sample was density separated at 2.58 g/

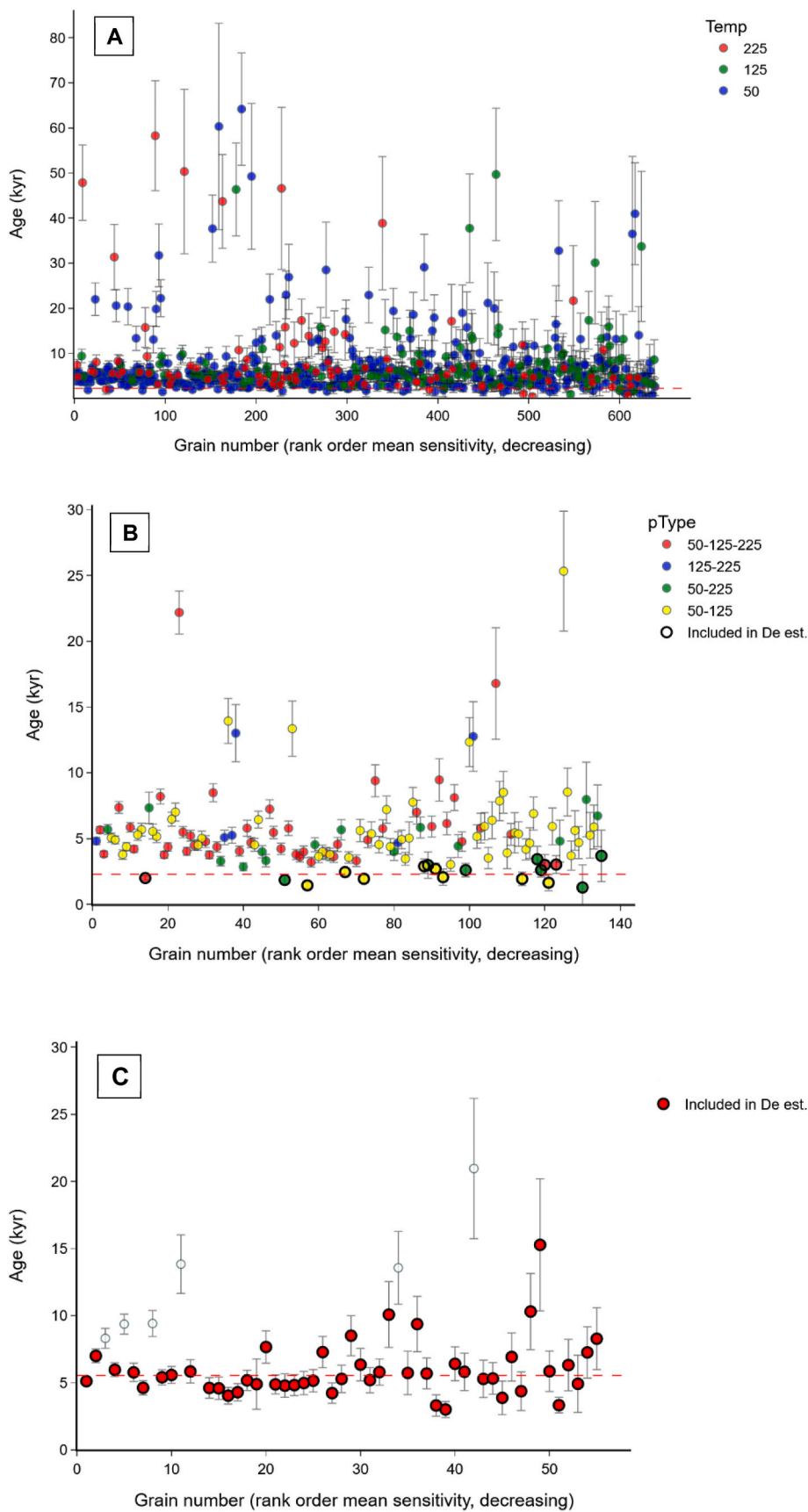


Fig. 1. 3ET filters illustrated by a sample from El Paso Peaks (J0156). (A) IRSL measurements are made at three elevated temperatures: 50, 125, and 225 °C. (B) 3ET All temperature points (3ET-ATP): Plateau D_E values at each temperature are combined for each grain. A minimum age model is then applied to this filtered subset of plateau grains for estimating the final D_E . (C) 3ET High temperature points (3ET-HTP): Plateau D_E values are based only on those signals that were reset across 125 and 225 °C. No fading corrections have been applied to these measurements (see text for discussion).

cm³ to separate quartz from feldspar. The lighter feldspar fraction was given a second sieve to separate out the 180–212 μm fraction which was used for dating.

Single-grain 3ET measurements were made on a Risø TL-DA-20D DASH single grain reader using a single-aliquot regenerative dose protocol (Table 2). The detection filters used were a Risø blue filter pack, comprising a Schott BG3 and BG39 combination. The IR LED power was about 150 mW cm⁻² at the sample position and the IR laser power about 450 mW cm⁻². Blue LED power used for bleaching tests was about 80 mW cm⁻² at sample. Signals were integrated over the first 0.5 s of stimulation and background values were determined by integrating over a window 2.0–2.5 s after initial stimulation. All steps were performed first for the natural signal and then repeated for each dose in a series of laboratory-applied doses. To expedite processing of the large data sets produced by the 3ET protocol, we developed code using Python along with open-source software packages for data analysis and visualization. In a Jupyter notebook environment (Kluyver et al., 2016) we used the Pandas data analysis library (McKinney, 2011) and Plotly graphing package (Plotly Technologies Inc, 2015) to apply the 3ET filter and to render the resulting data in interactive visualizations.

Growth curves of luminescence signals, normalized as Lx/Tx values versus dose were fit for individual grains with an exponential-plus-linear curve to determine an equivalent dose (D_E) for each grain at each of three IRSL measurement temperatures (50, 125, and 225 °C). The 3ET filtering algorithm compares a grain's D_E estimates across these three temperature points. Consistent D_E values are averaged into a single, 'plateau' D_E value, designated as either a 50–125, 50–225, 125–225, or 50–125–225 plateau. These 'plateau' grains are filtered for and passed through a discrete minimum age model using the algorithm developed for single grain pIRIR₂₂₅ age estimates (Rhodes, 2015; Rhodes and Walker, 2019). This approach is referred to as the 3ET-ATP (all temperature points) method as it includes values from all three specified temperature points. The 3ET-HTP (high temperature points) approach uses only 125 °C and 225 °C temperature points, excluding the less stable 50 °C D_E values. The concept behind this is to select those grains that were bleached sufficiently to zero both the 125 °C and 225 °C signals.

So to summarize:

3ET-ATP (all temperature points) is based on the 50, 125, and 225 °C signals.

3ET-HTP (high temperature points) is based on the 125, 225 °C signals only.

We determined fading rates based on combined data from six hundred single grains from sample Shfd19134, and measured g-values of 2.9 ± 1.2% per decade for the 50 °C, 1.0 ± 0.9% for 125 °C and 1.0 ± 1.0% for 225 °C. For this study, we included the data at each temperature without any fading corrections, as in the main, our single grain fading data demonstrated a range of small g-values. In principle, the 3ET approach may exclude grains with significant fading of the 50 °C signal, as these values may not form a plateau even if they were well bleached; however, see the discussion of this point below for sample J0156 from El Paso Peaks.

In addition to the 3ET age estimates, apparent ages were also calculated for D_E values at each of the three temperatures using the same approach as that used in single grain pIRIR₂₂₅ dating (Rhodes, 2015). Each of these apparent ages was derived from the full set of D_E values at the temperature under consideration not incorporating any information from other temperature signals. Analysis starts with all D_E values determined for that temperature that passed quality criteria, with high outliers rejected in turn until an internally consistent group of dose values remains. An overdispersion (sigma_b) value of 15% was used in these analyses. Fig. 1 illustrates the application of the 3ET protocol for a sample from El Paso Peaks, California.

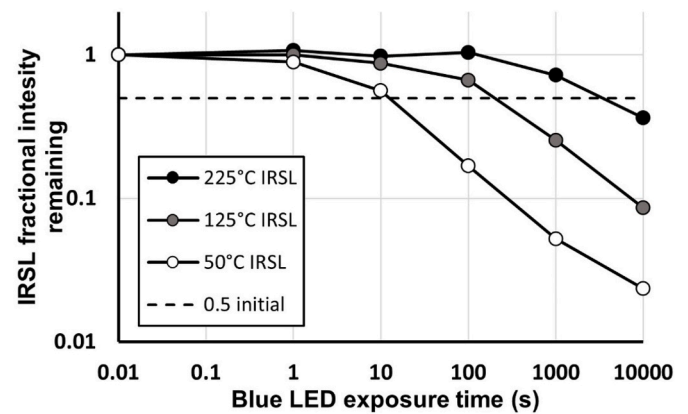


Fig. 2. Bleaching curves for sample Shfd19136 from the higher terrace on McLean Stream. Note that the y-axis uses a logarithmic scale. The horizontal dashed line indicates IRSL at half the initial intensity.

Table 3

Apparent ages and uncertainties (kyr before 2020 CE). Estimates are based on signals measured at each of three temperatures, then using 3ET methods.

Lab Code	50 °C	125 °C	225 °C	3ET-ATP	3ET-HTP
J0140	0.47 ± 0.03	0.55 ± 0.06	0.53 ± 0.08	0.46 ± 0.03	0.48 ± 0.06
	0.70 ± 0.03	0.97 ± 0.06	0.99 ± 0.07	0.75 ± 0.04	0.95 ± 0.06
J0150	1.32 ± 0.06	1.69 ± 0.13	1.51 ± 0.15	1.63 ± 0.09	1.76 ± 0.16
	3.25 ± 0.13	5.52 ± 0.24	5.36 ± 0.26	2.43 ± 0.17	5.55 ± 0.26
Shfd19126	0.35 ± 0.05	0.65 ± 0.11	1.00 ± 0.27	0.87 ± 0.17	2.73 ± 0.29
	0.89 ± 0.08	1.74 ± 0.16	2.79 ± 0.26	1.19 ± 0.17	1.48 ± 0.29
Shfd19128	1.39 ± 0.11	2.25 ± 0.19	3.16 ± 0.27	2.45 ± 0.21	2.82 ± 0.29
	0.28 ± 0.06	0.61 ± 0.14	0.81 ± 0.22	0.63 ± 0.08	0.64 ± 0.14
Shfd19130	0.61 ± 0.06	1.25 ± 0.11	2.18 ± 0.20	1.10 ± 0.11	2.30 ± 0.23
	4.06 ± 0.27	4.88 ± 0.33	5.27 ± 0.36	4.66 ± 0.31	4.91 ± 0.34
Shfd19132	2.34 ± 0.22	4.59 ± 0.35	4.55 ± 0.38	1.69 ± 0.34	3.97 ± 0.36
	1.62 ± 0.16	2.63 ± 0.28	4.10 ± 0.38	1.63 ± 0.21	3.66 ± 0.36
Shfd19134	2.34 ± 0.19	4.43 ± 0.33	5.40 ± 0.42	1.80 ± 0.28	2.32 ± 0.46
	2.98 ± 0.26	2.46 ± 0.48	5.92 ± 0.51	5.29 ± 0.42	5.24 ± 0.53
Shfd19136	5.01 ± 0.51	6.87 ± 1.04	4.19 ± 1.37	4.55 ± 0.65	3.96 ± 1.17
	4.06 ± 0.31	5.30 ± 0.44	7.43 ± 0.61	3.60 ± 0.38	5.36 ± 0.51

4. Results

Bleaching tests for a sample from New Zealand (Shfd19136) illustrate differences in the bleachability of IRSL signals measured at different temperatures using blue wavelengths (Fig. 2). Electron traps emptied during IRSL stimulation at higher temperatures are more stable and less quickly bleached by sunlight exposure than traps emptying at lower temperatures (Kars et al., 2014a). Blue LED bleaching times in a Risø DASH unit at 90% power to reduce the IRSL signal to below 10% of its initial intensity are on the order of 300 s (5 min) for the 50 °C IRSL signal; 7000 s (2 h) for the 125 °C signal; and 400,000 s (equivalent to about 9 days of daylight exposure) for the 225 °C signal. The differential bleachability of IRSL signals across temperatures suggests that

Table 4

3ET age estimates and radiocarbon age ranges for stratigraphic units at El Paso Peaks site. The radiocarbon age ranges listed here are based on ranges listed in Dawson et al. (2003). These estimates are for stratigraphic units or events rather than for individual samples and are based on a Bayesian analysis of the entire set of calibrated ages. Relevant radiocarbon sample numbers and ages are listed in Table 1 of Dawson et al. (2003). The resulting age ranges have here been converted to years before 2020 CE in order to be directly comparable to the luminescence age estimates.

Stratigraphic unit/event	Basis of estimate	Luminescence sample lab code	Radiocarbon-based age ranges and luminescence ages (years before 2020 CE)
Unit 98	Radiocarbon	–	410–310; 300–200
Unit 100	3ET-HTP	J0140	480 ± 60
Unit 102	Radiocarbon	–	520–360
Event U	Radiocarbon	–	960–590
Unit 128b	3ET-HTP	J0145	950 ± 60
Unit 132	Radiocarbon	–	1780–1490
Unit 138	Radiocarbon	–	1600–1380
Unit 144	3ET-HTP	J0150	1760 ± 160
Unit 164	Radiocarbon	–	2070–1800
Unit 254	Radiocarbon	–	5520–4970
Unit 270	3ET-HTP	J0156	5550 ± 260
Unit 316	Radiocarbon	–	6380–6060

measuring IRSL at multiple temperatures can be used as an indicator for the completeness of bleaching. Note that these experiments were performed using blue LEDs, but a direct comparison between samples bleached with natural California sunlight and these same blue LEDs demonstrated a similar bleaching rate for the MET-IRSL signal at 140 °C (Rhodes and Leathard, this volume, in press). Under natural conditions, the wavelengths and intensity incident on grains during transport in fluvial systems depends on many factors including water depth and suspended sediment load, as well as weather conditions and time of day, so referring observed bleaching characteristics to standardized reproducible conditions is probably a useful approach.

Four samples from near El Paso Peaks were tested for consistency of 3ET age estimates with independent age estimates by radiocarbon (Tables 3 and 4, and Fig. 3). In all samples the resulting 125 °C ages and the 3ET-HTP ages are consistent with radiocarbon results, covering a range of between about 500 and 5500 years ago. In three of the four samples the 125 °C, 225 °C, 3ET-ATP, and 3ET-HTP ages are all consistent with ages based on radiocarbon.

The twelve samples from the McLean Stream site suggest a similar age range as that covered by the El Paso Peak samples. Although on average apparent ages are older for higher terraces, these age estimates are quite variable and demonstrate some inconsistencies both within and across terraces (Table 3 and Fig. 4). Moreover, sand from the modern channel which was known from previous field observations to have been deposited within the last few years fails to produce an estimate that is statistically consistent with a zero age. As discussed below,

however, the minimum 3ET-HTP ages for each terrace do produce an internally consistent set of apparent ages in proper sequence.

5. Discussion

Does the 3ET method produce reliable age estimates? The four samples from a paleoseismic trench near El Paso Peaks demonstrate that the 3ET-HTP method produces reliable age estimates for samples ranging from ~500 to ~5000 years old. In one case (sample J0156) the 3ET-ATP age estimate is affected by the inclusion of 50 °C points that caused an underestimate of the age. This is possibly due to fading of the 50 °C signal. We examined the signals from the grains responsible for this apparent underestimate, and in each case the 125 °C or 225 °C D_E estimate involved in the plateau was significantly higher than that from 50 °C for the respective grain, but had a greater uncertainty, allowing the D_E value to be drawn down by the more precise 50 °C estimate. For the El Paso Peak samples, the agreement in age estimates between the 125 °C and 225 °C signals demonstrates thorough bleaching occurred prior to the most recent burial event for the selected grains, while those showing differences in apparent age were rejected.

The twelve samples from McLean Stream, New Zealand are more difficult to interpret. The range of apparent ages for a given terrace suggests that incomplete bleaching is a problem for these samples, with many of the ages being over-estimates due to poorly bleached grains. Unlike the El Paso Peak samples, there is disagreement between the 125 °C ages and the 3ET ages. We take the most likely age for each terrace as the minimum value of the 3ET-HTP plateau ages among samples from a given terrace. This minimum 3ET-HTP age represents grains that were bleached sufficiently at the last exposure event to reset both 125 and 225 °C signals. On the lowest terrace for instance, sample Shfd19129 has consistent values for 125 °C, 225 °C, and 3ET ages, all at a lower age estimate than for any of the other three samples from that terrace. Based on the apparent age distributions, it is likely that the other three samples received only enough sunlight to partially reset the 50, 125, and 225 °C signals. As expected, bleaching was more thorough for lower temperature signals. Assigning ages based on the minimum 3ET-HTP result for each terrace produces an internally consistent sequence of increasing age for successively higher terraces.

The difference in bleaching environments of the two study catchments is likely a primary control on the differences in luminescence behaviors observed between the two sites (Table 5). The El Paso Peaks site lies in a playa fed by a small catchment in a low energy desert environment with abundant sunshine. In contrast, McLean Stream occupies a narrow valley that opens immediately at the study transect where it enters the wider Clarence River valley. Sand grains in these terraces will have traveled at most 6 km from their source areas, following steep gradients through constricted valleys and bordered by slopes that contribute freshly eroded sediment to the system. Therefore, there are minimal opportunities for exposure to sunlight for bleaching of IRSL signals for these terraces.

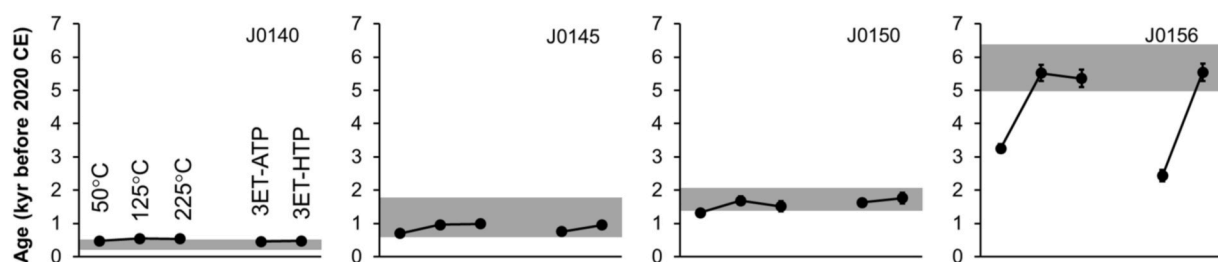


Fig. 3. Luminescence apparent ages for four samples from the trench at El Paso Peaks (represented as points) with expected ages for the target strata (represented by the shaded areas). Points represent apparent luminescence ages, from left to right: 50 °C, 125 °C, 225 °C, 3ET-ATP, and 3ET-HTP calculated ages. For some points the error bars are smaller than the symbol and thus not visible at this scale. The shaded zones are based on expected ages as reported in Dawson et al. (2003). The older boundary is the maximum of the age range estimated for the underlying stratigraphic unit, and the younger boundary is the minimum of the age range estimated for the overlying unit. All ages are expressed in kyr before 2020 CE.

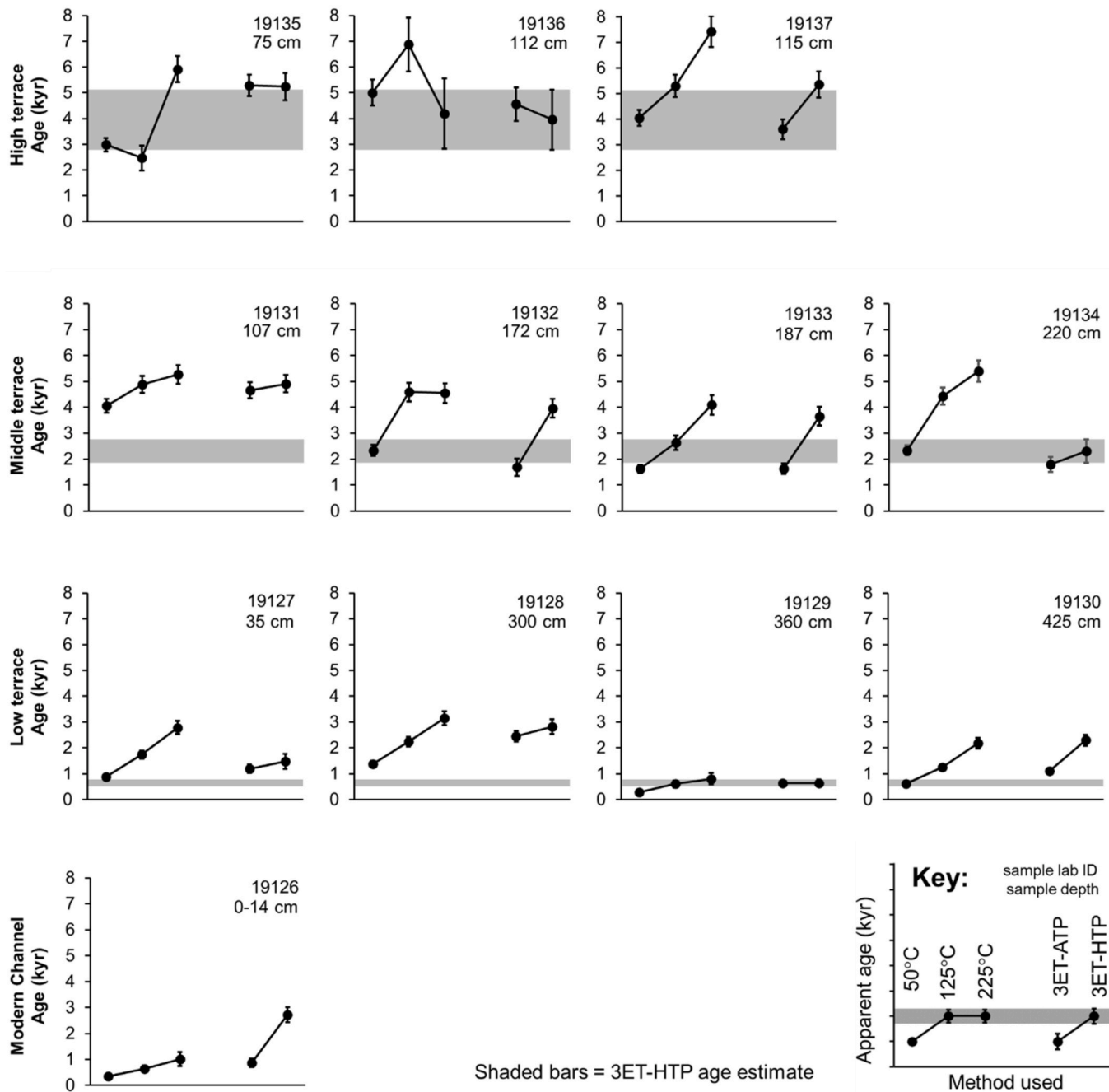


Fig. 4. Apparent ages for McLean Stream terraces and modern channel. Each of three terraces were sampled at multiple depths. For each chart the y-axis represents age in thousands of years prior to 2020 CE. The five points plotted are from left: 50 °C, 125 °C, 225 °C, 3ET-ATP, and 3ET-HTP apparent ages. Note: Shaded bars represent the most likely age of the terrace as based on the minimum 3ET-HTP age determined for a particular terrace.

The difference in bleaching between the two catchments is illustrated by comparing the number of saturated grains from the uppermost sample at El Paso Peaks with the modern stream sample at McLean Stream (Table 6). For this analysis, we considered saturated grains to be those with D_E values greater than $2D_0$. Only a few percent of grains at the El Paso Peaks site are still saturated after traversing the catchment, whereas many grains in the modern McLean Stream channel remain saturated. The number of saturated grains is higher for the higher temperature signals, with 63% of the 225 °C signals remaining saturated in McLean Stream.

The percentage of saturated grains is an index of bleaching and helps

confirm that few grains in the McLean Stream catchment received adequate sunlight exposure during transport—they are unlikely even to have received enough sunlight to distinguish their luminescence signal from that of never-exposed bedrock grains. Thus, it is to be expected that many hundreds of grains must be measured to have a probability of encountering a few with a 225 °C IRSL signal that is completely bleached. For the middle terrace, a total of 3600 grains were measured, of which three (in Shfd19134) are included in the 3ET-HTP age estimate that most likely reflects the most recent bleaching event. In the case of Shfd19134, an evaluation based solely on the pIRIR₂₂₅ apparent age would possibly have missed the appropriate age estimate.

Table 5

Comparison of the two study catchments, including factors that can influence grain bleachability.

Characteristic	El Paso Peaks site, USA	McLean Stream, NZ
Catchment Area above site	0.38 km ²	10.2 km ²
Highest Elevation	1158 m	1198 m
Elevation at site/transect	1010 m	111 m
Local Relief	148 m	1087 m
Longest drainage in catchment	1.3 km	5.8 km
Average stream gradient	11%	19%
Precipitation/yr (average)*	144	967
Sunny hours/yr (average)*	3882	2909
Vegetation cover	Sparse; desert shrubs	Dense

*Source: climate-data.org

Table 6

Percentage of saturated grains out of 600 grains measured.

	El Paso Peaks (J0140)			McLean Stream (Shfd19126)		
	50 °C	125 °C	225 °C	50 °C	125 °C	225 °C
IRSL signal measurement temperature						
Grains with valid growth curves	328	143	98	375	334	313
Saturated Signals	8	5	14	50	144	196
Grains saturated (percent)	2.4	3.5	14.3	13.3	43.1	62.6

One difficulty in applying the 3ET method for samples with restricted bleaching is that the 3ET filtering algorithm by necessity even further reduces the number of grains available for the analysis, increasing the sensitivity of the result to the characteristics of individual grains. One way to compensate for so few results is to collect multiple samples and to use the stratigraphic and geomorphic context of each to help evaluate the reliability of the set of samples as a whole.

The way we have established the 3ET method, using the same pre-heating as our regular single grain pIRIR₂₂₅ approach, and also maintaining IRSL measurements at 50 and 225 °C, renders this effectively an experiment that includes data we could interpret in the usual manner, though recognizing differences in the bleaching rate of the 225 °C signal when measured following two prior IRSL exposures (at 50 and 125 °C). The method acts as a filter allowing only well bleached grains to be included for consideration in age determination. One specific reason for this is to minimize “shadowing”, a term introduced by Rhodes and Walker (2019). Shadowing can be caused when a significant population of partially bleached grains with apparent equivalent doses greater than that reflecting the true depositional age leads to the smaller number of well bleached results with slightly lower values being interpreted simply as low-side values for a distribution that includes all of these results, well bleached and partially bleached. By excluding the partially bleached grains, a clearer picture of the populations of well bleached grains can emerge. In some cases, shadowing can be caused by the inclusion of reworked grains that were well bleached during an earlier catchment event relatively closely spaced in time such that equivalent dose uncertainty values from this event and the slightly younger true depositional age overlap. In this case, no statistical approach is likely to be able to differentiate these two events.

Our sampling and luminescence measurement strategy here and at other sites (e.g., Zinke et al., 2017) includes the collection and measurement of multiple samples for each target event, typically three to five samples arranged in a short vertical sequence from a single pit or exposure. The reason for this approach is because we detect wide variations in the degree of prior bleaching for grains from closely spaced samples (e.g., see the data presented by Zinke et al., 2017); this is likely due to the timescales of grain transport and deposition in moderate to high energy fluvial systems. We expect that approximately 50% of

samples were deposited when sunlight was absent; high topography, turbid water and storm clouds all further reduce the likelihood of direct sunlight bleaching, so probably most bleaching occurred in days, weeks and years before deposition occurred, rather than during the final transport. When high flows occur, we also expect significant erosion of river banks, older fluvial terraces and material on surrounding hillslopes with a significant input of unbleached or partially bleached grains. In a complex situation such as this, we consider that any individual sample may include a greater or lower proportion of grains that were well bleached at the time of deposition. By measuring multiple samples, we consider that we also increase the probability of finding a relatively well bleached sample that can provide a secure age estimate for the target event. The single grain 3ET approach requires us typically also to measure a larger number of grains for each sample dated than using SG pIRIR₂₂₅ dating, helping to better quantify the D_E distributions observed and so better understand the bleaching history of this population of grains.

A benefit of the 3ET method is the insight it gives into the thoroughness of bleaching for individual grains that is lacking in traditional single grain pIRIR protocols. Samples with a consistent apparent age across 50, 125, and 225 °C measures and at both 3ET measures are more likely to reflect a real bleaching event. Sample Shfd19129 from the low terrace is perhaps the best example of a well bleached sample from the McLean Stream terraces, confirmed by nicely consistent 3ET measurements. In contrast, inconsistent apparent ages, as illustrated for example by the three samples from the upper McLean Stream terrace, can mark poorly bleached samples as less reliable for constraining the age of the last depositional event. Thus, the 3ET approach is an insightful indicator of sample reliability, yielding evidence that can flag poorly bleached samples as less reliable while helping to confirm the robustness of well bleached samples.

6. Conclusions

In this paper we introduce the 3ET method, a simplified MET protocol based on three measurement temperatures (50, 125, and 225 °C). The 3ET method computes a D_E value for a sample by filtering for grains which have D_E ‘plateaus’ across temperatures for an individual grain. Age estimates are then based either on all three measurements (3ET-ATP, for all temperature points) or on the higher two temperature measurements only (3ET-HTP, for high temperature points). The central aim of the 3ET method is to filter out grains that have been incompletely bleached, taking grains with consistent D_E values across temperatures as indicative of a thorough bleaching event.

We evaluated this approach using two sets of samples with independent age information. First, we tested a set of well bleached samples from California that had been rigorously dated with independent radiocarbon age estimates. For these samples the 3ET-HTP method produced reliable age estimates spanning an age range of ~500 to ~5000 years. Secondly, we tested a set of more poorly bleached samples from a sequence of fluvial terraces in New Zealand. These samples lack absolute, independent age control but are dated relative to one another as ages increase for each successively higher terrace. For these terraces, the 3ET-HTP method produced an internally consistent set of age estimates, with some limitations. In a few cases, lower 50 °C D_E values affect the 3ET-ATP age estimates by making them too young, possibly due to unreliability in the 50 °C signals compared to the more stable signals at higher temperature. Therefore, the 3ET-HTP age estimates are considered more reliable.

The small number of well bleached grains in the samples from New Zealand required a high number of grains to be measured and therefore longer machine measurement times. In settings where bleaching is similarly restricted by environmental or depositional conditions, collecting multiple samples for each targeted deposit or dating event can help to ensure that some well bleached grains can be included. Moreover, samples are usually not uniformly poorly bleached, so running

more samples increases the chances of finding samples that are well bleached and give clear, precise age estimates. Another benefit of this strategy is that simple stratigraphic coherence can be tested with multiple samples but can't with single samples.

This study has evaluated the 3ET method in two very different environments that represent end members in degree of bleaching. Future application of 3ET in other settings will help to further evaluate the benefits and limitations of the technique. In settings where incomplete bleaching may be of concern, the 3ET technique gives another means for evaluating the degree of bleaching for individual grains and a way to filter out those grains that are likely to have been incompletely bleached. More generally, the 3ET method can serve as a reliability indicator that can flag poorly bleached samples as potentially unreliable while helping to confirm well bleached samples as more reliable for robust age determinations.

Declaration of competing interest

The authors declare that they have no known competing financial interests or personal relationships that could have appeared to influence the work reported in this paper.

Acknowledgements

Thanks to Belinda Roder and Bryan Anderson for field and laboratory assistance for El Paso Peaks samples, and to Rob Ashurst and Jane Leathard for laboratory assistance with New Zealand samples. We thank landowners and residents in the Clarence Valley who provided access, support, and advice. Thanks also to Tom Nicholson for assistance with data analysis and to Wesley Ivester for advice on coding with Python.

We acknowledge funding from SCEC award #11198, NERC award NE/S007091/1 and NSF Award Number 1759252.

References

- Banerjee, D., Murray, A.S., Bøtter-Jensen, L., Lang, A., 2001. Equivalent dose estimation using a single aliquot of polymineral fine grains. *Radiat. Meas.* 33, 73–94.
- Buylaert, J.-P., Jain, M., Murray, A.S., Thomsen, K.J., Thiel, C., Sohbati, R., 2012. A robust feldspar luminescence dating method for Middle and Late Pleistocene sediments. *Boreas* 41, 435–451. <https://doi.org/10.1111/j.1502-3885.2012.00248.x>. ISSN0300-9483.
- Buylaert, J.P., Murray, A.S., Thomsen, K.J., Jain, M., 2009. Testing the potential of an elevated temperature IRSL signal from K-feldspar. *Radiat. Meas.* 44, 560–565.
- Colarossi, D., Duller, G.A.T., Roberts, H.M., 2018. Exploring the behaviour of luminescence signals from feldspars: implications for the single aliquot regenerative dose protocol. *Radiat. Meas.* 109, 35–44.
- Dawson, T.E., McGill, S.F., Rockwell, T.K., 2003. Irregular recurrence of paleoearthquakes along the central Garlock fault near El Paso Peaks, California. *J. Geophys. Res. Solid Earth* 108 (B7).
- Fu, X., Li, S.H., 2013. A modified multi-elevated-temperature post-IR IRSL protocol for dating Holocene sediments using K-feldspar. *Quat. Geochronol.* 17, 44–54. <https://doi.org/10.1016/j.quageo.2013.02.004>.
- Kars, R.H., Reimann, T., Ankjaergaard, C., Wallinga, J., 2014a. Bleaching of the post-IR IRSL signal: new insight for feldspar luminescence dating. *Boreas* 43, 780–791.
- Kars, R.H., Reimann, T., Wallinga, J., 2014b. Are feldspar SAR protocols appropriate for post-IR IRSL dating? *Quat. Geochronol.* 22, 126–136. <https://doi.org/10.1016/j.quageo.2014.04.001>.
- Kluyver, T., et al., 2016. Jupyter Notebooks – a publishing format for reproducible computational workflows. In: Loizides, F., Schmidt, B. (Eds.), *Positioning and Power in Academic Publishing: Players, Agents and Agendas*, pp. 87–90.
- Li, B., Li, S.H., 2011. Luminescence dating of K-feldspar from sediments: a protocol without anomalous fading correction. *Quat. Geochronol.* 6 (5), 468–479.
- McGuire, C.P., Rhodes, E.J., 2015. Downstream MET-IRSL single-grain distributions in the Mojave River, southern California: testing assumptions of a virtual velocity model. *Quat. Geochronol.* 30, 239–244.
- McKinney, W., 2011. pandas: a foundational Python library for data analysis and statistics. *Python High Perform. Sci. Comput.* 14 (9), 1–9.
- Plotly Technologies Inc, 2015. Collaborative Data Science. Montréal, QC. <https://plot.ly>.
- Rhodes, E.J., 2015. Dating sediments using potassium feldspar single-grain IRSL: initial methodological considerations. *Quat. Int.* 362, 14–22. <https://doi.org/10.1016/j.quaint.2014.12.012>.
- Rhodes, E.J., & Leathard J.A. (in press), this volume) MET-IRSL used to track pre-depositional sediment transport history. *Quat. Geochronol.*
- Rhodes, E.J., Walker, R.T., 2019. Applications of luminescence dating to active tectonic contexts. In: Bateman, M.D. (Ed.), *Handbook of Luminescence Dating*. Whittles publishing, Caithness, UK, pp. 293–320.
- Reimann, T., Tsukamoto, S., Naumann, M., Frechen, M., 2011. The potential of using K-rich feldspars for optical dating of young coastal sediments – a test case from Darss-Zingst peninsula (southern Baltic Sea coast). *Quat. Geochronol.* 6, 207–222.
- Reimann, T., Thomsen, K.J., Jain, M., Murray, A.S., Frechen, M., 2012. Single-grain dating of young sediment using the pIRIR signal from feldspar. *Quat. Geochronol.* 11, 28–41. <https://doi.org/10.1016/j.quageo.2012.04.016>.
- Reimann, T., Notenboom, P.D., De Schipper, M.A., Wallinga, J., 2015. Testing for sufficient signal resetting during sediment transport using a polymineral multiple-signal luminescence approach. *Quat. Geochronol.* 25, 26–36.
- Roder, B.J., Lawson, M.J., Rhodes, E.J., Dolan, J.F., McAuliffe, L., McGill, S.F., 2012. Assessing the potential of luminescence dating for fault slip rate studies on the Garlock fault, Mojave Desert, California, USA. *Quat. Geochronol.* 10, 285–290. <https://doi.org/10.1016/j.quageo.2012.03.013>.
- Smedley, R.K., Duller, G.A.T., 2013. Optimising the reproducibility of measurements of the post-IR IRSL signal from single-grains of feldspar for dating. *Anc. TL* 31 (2), 49–58.
- Smedley, R.K., Buylaert, J.-P., Ujvari, G., 2019. Comparing the accuracy and precision of luminescence ages for partially-bleached sediments using single grains of K-feldspar and quartz. *Quat. Geochronol.* 53, 101007. <https://doi.org/10.1016/j.quageo.2019.101007>.
- Thomsen, K.J., Murray, A.S., Jain, M., Bøtter-Jensen, L., 2008. Laboratory fading rates of various luminescence signals from feldspar-rich sediment extracts. *Radiat. Meas.* 43, 1474–1486.
- Zinke, R., Dolan, J.F., Rhodes, E.J., Van Dissen, R., McGuire, C.P., 2017. Highly variable latest pleistocene–holocene incremental slip rates on the Awatere fault at Saxton river, South Island, New Zealand, revealed by Lidar mapping and luminescence dating. *Geophys. Res. Lett.* 44 <https://doi.org/10.1002/2017GL075048>.